Title: Mediterranean cyclogenesis in phase with African monsoon strength during past 1.36 million years

Authors: Bernd Wagner[1]*†, Hendrik Vogel[2]†, Alexander Francke[1,3], Tobias Friedrich[4], Timme Donders[5], Jack Lacey[6,7], Melanie Leng[6,7], Eleonora Regattieri[8,9], Laura Sadori[10], Thomas Wilke[11], Giovanni Zanchetta[8], Christian Albrecht[11], Adele Bertini[12], Nathalie Combourieu-Nebout[13], Aleksandra Cvetkoska[5, 11], Biagio Giaccio[14], Andon Grazhdani[15], Torsten Hauffe[11], Jens Holtvoeth[16], Sebastien Joannin[17], Elena Jovanovska[11], Janna Just[1,18], Katerina Kouli[19], Ilias Kousis[20], Andreas Koutsodendris[20], Sebastian Krastel[21], Niklas Leicher[1], Zlatko Levkov[22], Katja Lindhorst[21], Alessia Masi[10], Martin Melles[1], Anna M. Mercuri[23], Sebastien Nomade[24], Norbert Nowaczyk[25], Konstantinos Panagiotopoulos[1], Odile Peyron[17], Jane M. Reed[26], Leonardo Sagnotti[27], Gaia Sinopoli[10], Björn Stelbrink[11], Roberto Sulpizio[28, 29], Axel Timmermann[30,31], Slavica Tofilovska[22], Paola Torri[32], Friederike Wagner-Cremer[5], Thomas Wonik[33], Xiaosen S. Zhang[34]

Affiliations:

[1]Institute of Geology and Mineralogy, University of Cologne, Cologne, Germany.

[2]Institute of Geological Sciences & Oeschger Centre for Climate Change Research, University of Bern, Bern, Switzerland.

[3]Wollongong Isotope Geochronology Laboratory, University of Wollongong, Wollongong, Australia.

[4]International Pacific Research Center, University of Hawaii at Manoa, Honolulu, Hawaii 96822, USA.

[5]Palaeoecology, Department of Physical Geography, Utrecht University, Utrecht, The Netherlands.

[6]Centre for Environmental Geochemistry, School of Geography, University of Nottingham, Nottingham, UK.

[7]NERC Isotope Geosciences Facilities, British Geological Survey, Keyworth, Nottingham, UK.

[8]Dipartimento di Scienze della Terra, University of Pisa, Pisa, Italy.

[9]Institute of Earth Sciences and Earth Resources-Italian National Research Council (IGG-CNR), Pisa, Italy.

[10]Dipartimento di Biologia Ambientale, Università di Roma "La Sapienza", Rome, Italy.

[11]Department of Animal Ecology & Systematics, Justus Liebig University Giessen, Giessen, Germany.

[12]Dipartimento di Scienze della Terra, Università di Firenze, Firenze, Italy.

[13]CNRS UMR 7194, Muséum National d'Histoire Naturelle, Institut de Paléontologie Humaine, Paris, France.

[14]Istituto di Geologia Ambientale e Geoingegneria – CNR, Rome, Italy.

[15]Faculty of Geology and Mineralogy, University of Tirana, Albania.

[16]School of Chemistry, University of Bristol, Bristol, UK.

[17]CNRS UMR 5554, Institut des Sciences de l'Evolution de Montpellier, Université deMontpellier, Montpellier, France.

[18]Fachbereich Geowissenschaften, Universität Bremen, Bremen, Germany.

[19]Faculty of Geology and Geoenvironment, National and Kapodistrian University of Athens, Athens, Greece.

[20]Paleoenvironmental Dynamics Group, Institute of Earth Sciences, Heidelberg University, Heidelberg, Germany.

[21]Institute of Geosciences, Christian-Albrechts-Universität zu Kiel, Kiel, Germany.

[22]University Ss Cyril and Methodius, Institute of Biology, Skopje, FYROM.

[23]Dipartimento di Scienze della Vita, Laboratorio di Palinologia e Paleobotanica, Università di Modena e Reggio Emilia, Modena, Italy.

[24]Laboratoire des Sciences du Climat et de l'Environnement, UMR 8212, CEA/CNRS/UVSQ et Université Paris-Saclay 91198 Gif-Sur-Yvette, France.

[25]Helmholtz Centre Potsdam, GFZ German Research Centre for Geosciences, Potsdam, Germany.

[26]Geography, School of Environmental Sciences, University of Hull, Hull, UK.

[27]Istituto Nazionale di Geofisica e Vulcanologia, Rome, Italy.

[28]Dipartimento di Scienze della Terra e Geoambientali, University of Bari, Bari, Italy.

[29]IDPA-CNR, Milan, Italy.

[30]Center for Climate Physics, Institute for Basic Science, Busan, South Korea

[31]Pusan National University, Busan, South Korea

[32]Dipartimento di Scienze della Vita, Laboratorio di Palinologia e Paleobotanica, Università di Modena e Reggio Emilia, Modena, Italy.

[33]Leibniz Institute for Applied Geophysics (LIAG), Hannover, Germany.

[34]Institute of Loess Plateau, Shanxi University, Taiyuan, China.

*Correspondence to: wagnerb@uni-koeln.de.

† these authors contributed equally to this work.

Abstract: Rainfall is a key climatic factor for socioeconomic development in densely populated and summer dry regions such as the Mediterranean borderlands. However, the drivers for rainfall variability are poorly constrained due to the lack of suitable climate archives, necessary to validate climate model data on Quaternary time-scales. Here we present a continuous rainfall proxy time-series from a sedimentary record from Lake Ohrid spanning the last 1.36 million

years. Our data suggest increased rainfall as a result of strong seasonal contrast in insolation during phases characterized by low continental ice volume and high atmospheric CO_2 concentrations. This is in excellent agreement with climate model data and indicates that maxima in Mediterranean cyclogenesis and convective precipitation are in phase with changes in African monsoon circulation.

One Sentence Summary: Lake Ohrid sediment record and climate simulation data depict Mediterranean rainfall variability during the Quaternary

Main Text:

Mediterranean climates are characterized by strong seasonal contrasts associated with dry and warm summers, and wet and mild winters. The amount of winter precipitation determines the prevailing type of vegetation and water availability, and has strong socioeconomic implications in this densely populated region. In recent decades, winter droughts have become a widespread phenomenon in the Mediterranean borderlands, with anthropogenic greenhouse gas and aerosol forcing identified as potential contributors (*1*). Current climate model simulations, using the Representative Concentration Pathways (RCP) 4.5, 8.5 scenarios, simulate a progressive summer drying over the next 82 years (*2*). Rainfall changes during the Northern Hemisphere (NH) winter months (October through March) are less well constrained, with different simulation runs showing either trends towards wetter or drier conditions. The uncertainty for projections in winter precipitation limits the extent to which current modelling approaches are useful for decision makers (*3*, *4*).

A major source of uncertainty in models is the lack of long-term, empirical baseline data. Proxy records and modelling experiments suggest that enhanced rainfall in the Mediterranean region is in phase with the northward shift of the intertropical convergence zone (ITCZ) and increase in African monsoon strength during Northern Hemisphere summer insolation (NHSI) maxima and winter insolation (NHWI) minima (*5*-*8*). However, most continental proxy records that are capable of capturing hydroclimate change do not cover multiple NHSI maxima with different underlying orbital geometries. In fact, the majority of records are restricted to the Holocene (*9*, *10*), yet the maximum in NHSI during the Early Holocene was relatively weak compared to most Quaternary interglacials due to lower eccentricity. Terrestrial proxy time-series covering multiple NHSI maxima from the Mediterranean region are scarce (e.g. *6*, *11*). Sediment records from the Mediterranean Sea provide continuity throughout the Plio-Pleistocene and capture cessations of deep-water ventilation associated with the formation of prominent, organic-rich sapropel layers (*12*, *13*). While multiple factors contribute to sapropel formation, increased freshwater input, particularly from the African continent during NHSI-forced monsoon maxima, is considered the most important (*14*, *15*). Hence, the Mediterranean sapropel record is thought to be an excellent indicator of the relative timing of increased African monsoon strength rather than a direct indicator of precipitation in, and runoff from, the entirety of the Mediterranean borderlands. Reconstructed rainfall increases in the northern Mediterranean borderlands during sapropel formation have been interpreted to be a product of both intensified summer and winter rainfall (*15*, *16*). Modelling experiments explain increased winter precipitation by stronger wintertime storm tracks (*6*) or air-sea temperature difference, and locally induced convective precipitation that dominate freshwater budget changes on obliquity time scales (*17*). Alternatively, conceptual models based on proxy time series have suggested

increases of the frequency and intensity of low-pressure systems evolving in the Mediterranean region, mostly during fall and early winter (*5*, *7*, *16*). Hence, a well-dated proxy record covering multiple glacial-interglacial cycles and being sensitive to changes in Mediterranean hydroclimate, is key to addressing long-standing questions regarding the underlying mechanisms, timing, and amplitude of rainfall variability under different climate boundary conditions (greenhouse gas (GHG) concentration, orbital geometries, continental ice sheet volume and extent).

Here we assess rainfall variability in a continuous, independently dated 1.36 Myr sediment core from Lake Ohrid in the Balkans (Fig. 1). Climate variations at this site represent broader variability in the northern Mediterranean borderlands (*18*). We compare our sedimentary proxy time-series with transient climate simulation data and monsoon records, to provide a comprehensive mechanistic understanding of rainfall variability and seasonality, as well as phase relationships to orbital-scale forcings.

Lake Ohrid, Europe's oldest and most biodiverse lake (*19*), is a 293-m-deep tectonic and hydrologically open lake, primarily fed by an extensive karst aquifer system, which supplies ions to the lake (mainly Ca^{2+} and HCO_3^-) and filters particulate matter (*20*). Scientific drilling of the lake in 2013 resulted in a 584-m-long composite sediment succession from the lake centre, comprising fine-grained hemi-pelagic muds in the upper 447 m (*21*, *22*). Sedimentation is thought to have been uninterrupted, as there is no evidence of unconformities or erosion surfaces. Independent age control from 13 interspersed tephra layers in combination with magnetostratigraphy provides a robust chronological framework. This framework allows us to match changes in orbital parameters with our proxy data for further refinement of age-depth relationships. The data demonstrate that the Lake Ohrid record spans the last ~1.36 Myr (Fig. 1; fig. S3).

Indicators for detrital input (quartz, potassium, titanium), catchment vegetation (arboreal pollen (AP, excluding pine), deciduous oaks), and hydrologic variability (total inorganic carbon (TIC) content, Ca/K, $\delta^{18}O_{calcite}$, $\delta^{13}C_{calcite}$) show clear orbital-scale cyclicity (Fig. 2; figs S7, S9, and S10), characterized by a strong precessional (~21 ka) component. During periods of global ice volume minima and NHSI maxima, we observe prominent peaks in the hydrological and vegetation proxy data (Fig. 2). We interpret these peaks in TIC (mainly from endogenic calcite) and Ca/K (a proxy for the concentration of endogenic calcite) as a result of enhanced activity of and ion supply from the karst aquifers combined with high productivity due to warmer conditions (*20*). Pollen show a simultaneous shift in vegetation structure towards a dense forest, with elevated amounts of deciduous oaks in the catchment, especially during early phases of interglacials, representing increased annual moisture availability. Lower $\delta^{13}C_{calcite}$ during these periods also suggests greater soil development and lower $\delta^{18}O_{calcite}$ (fig. S7) indicates a more positive precipitation/evaporation (P/E) balance (*23*). Thus, both aquatic and terrestrial datasets suggest extraordinary maxima in annual rainfall amount along with higher temperatures during interglacials.

To provide a better understanding of the observed rainfall variability from the Lake Ohrid record in a regional context, we analysed climate data time series derived from a transient LOVECLIM 784 ka GCM simulation (*24*, *25*) as well as NOAA reanalysis precipitation data of the Lake Ohrid region for the time period 1979-2017. Temperature time series of the 5°x5° Lake Ohrid grid cell simulated by the LOVECLIM earth system model closely resemble records of first-order global ice volume (fig. S7), such as the LR04 benthic oxygen isotope stack (*26*). The

close match to changes in the amount of detrital siliciclastics and tree pollen (AP-P) confirms the sensitivity of the Lake Ohrid record to global-scale climate fluctuations (Fig. 2; fig. S7). The highest amplitudes in precipitation time series occur during phases of reduced ice volume, with prominent peaks during NHSI maxima. The excellent conformity between simulated precipitation and our precipitation proxy time series emphasizes that the local response recorded at Lake Ohrid also captures changes in regional hydroclimate extending back to 1.36 Ma (Fig. 2).

Seen both, in paleo records and in climate model simulations, the intensification of NH monsoon systems during precession minima and peak NHSI is a prominent example for orbitally-forced changes in precipitation variability (*14*, *15*, *27*). Iconic records of monsoon strength, such as the Chinese speleothem (*27*), eastern Mediterranean sapropel (*12*, *13*, *28*) and planktonic foraminifera oxygen isotope records (*14*, *15*, *29*), show a strong positive phase relationship with Lake Ohrid hydrological proxy time series (Fig. 2). Strengthening of NH monsoons is associated with a northward displacement of atmospheric circulation systems, including the position of the Hadley cells and the ITCZ during NH summer. The shift of the Hadley cell amplifies subsidence over, and persistence of, high-pressure systems in the Mediterranean region, leading to warmer and drier summers (*17*) and higher sea-surface temperatures (SST) (*16*, *30*). Reduction of hemispheric insolation contrasts during the winter half-year results in a smaller equator to pole temperature gradient, southward-shifted northern Hadley and Ferrel cells, and weaker (and southward-shifted) mid-latitude westerlies. The observed relationship between the Lake Ohrid rainfall record (from TIC, Ca/K, deciduous oaks; Fig. 2, fig. S7) and the monsoon archives therefore requires increased precipitation during winter for the Lake Ohrid region.

The Lake Ohrid record, in combination with the transient simulation time-series and the NOAA reanalysis data, can provide fundamental insights into the mechanisms invoked by orbital forcing on Mediterranean rainfall. The monthly NOAA reanalysis data of the last 39 years show a distinct tendency for rainfall maxima (defined as above two standard deviations) to occur between the months of September to December (fig. S5A,B). The atmospheric pattern associated with the rainfall events exhibits a trough in the Gulf of Genova region (fig. S5C) pointing to increased cyclogenesis over the western Mediterranean region.

The annual cycle of simulated Lake Ohrid precipitation in LOVECLIM is in good agreement with the reanalysis data; the annual mean rainfall, however, is underestimated by the model (fig. S4B). Maxima in our precipitation simulation time series (defined as above two standard deviations) indicate a strong positive anomaly from September to November (SON) in agreement with the reanalysis data (Fig. 3, fig. S4B). The increase in SON precipitation is associated with the formation of a significant trough over the western Mediterranean (Fig. 3), whose formation requires relatively weak atmospheric stratification. The simulated atmospheric pattern is very similar to the one shown by the reanalysis data, providing us with confidence in our modelling approach. Our observations support previous modelling experiments suggesting that weakened atmospheric circulation and reduced hemispheric temperature contrasts (*6*), in combination with an increased contrast between warm SST and lower continental air temperatures (*17*), fuel precipitation increase in the Mediterranean mid-latitudes. Such a preconditioning is particularly pronounced at the beginning of fall, when the stronger thermal inertia of the sea relative to the land promotes moisture advection and cyclogenesis in the Mediterranean region (*31*). The increased cyclogenesis in the western Mediterranean appears to

be the main mechanism to explain an increased transport of moisture-bearing air masses to the Balkans and, in the wider sense, to Mediterranean mid-latitudes.

Owing to the strong coherency and agreement of the simulation with our proxy time-series, in terms of timing and amplitude during the last 784 kyr, we infer that this mechanism primarily controlled precipitation at Lake Ohrid over the last 1.36 Myr. Indeed, very similar to the NH summer monsoon records, we observe a strong influence of NHSI and a reduced winter temperature contrast in the NH throughout the entirety of our multiproxy time-series, suggesting persistence of the mechanism during fundamentally different climate boundary conditions. The positive phase relationship between the Lake Ohrid precipitation proxy time-series and sapropel records (Fig. 2) therefore infers a strong coherence of African summer monsoon strength and widespread Mediterranean fall precipitation. Some peaks in our precipitation proxy time series, which are not represented by sapropel layers (Fig. 2), may indicate lower monsoon strength and reduced runoff from the African continent or that the general setting required for sapropel deposition and preservation was not established in the Mediterranean Sea during these periods (*15*). During generally colder and drier glacial periods (*11*) with increased global ice volume, lower atmospheric CO_2 concentrations, and stronger mid-latitude westerlies, insolation forcing on precipitation appears suppressed in our record. This is in agreement with the sensitivity simulations conducted to disentangle the individual effects of orbital forcing, NH ice sheets and CO_2 on Lake Ohrid precipitation (Supplementary Materials). This points to a reduced frequency of cyclogenesis and convective precipitation as a result of an increased temperature contrast during NH winter months and/or lower sensitivity of our sedimentary proxies during colder, glacial climate states (*20*).

Precessional forcing on insolation is not only the key driver of the NH monsoons, it also exerts a strong control on rainfall variability in the Mediterranean mid-latitudes during the Quaternary. Lake Ohrid sediment cores record highly resolved, and chronologically well-constrained, information on rainfall maxima during phases of lower intrahemispheric temperature contrast and peak SST's over the last 1.36 Myr in exquisite detail. A reduced temperature contrast, particularly during the winter months, and an increase of Mediterranean SST's is also predicted for future climate scenarios. While the climate forcing of these scenarios is almost entirely related to the continued anthropogenic increase of atmospheric greenhouse gas concentrations, the impacts on the key drivers of rainfall amount in the Mediterranean are very similar to precessional forcing in the past. The Lake Ohrid rainfall record therefore provides an observational time-series that allows validation of regional scale climate simulations and may help to reduce simulation uncertainties for the Mediterranean.

References and Notes:

1. M. Hoerling, J. Hurrell, A. Kumar, L. Terray, J. Eischeid, P. Pegion, T. Zhang, X. Quan, T. Xu, On North American Decadal Climate for 2011–20. *J. Climate* **24**, 4519−4528 (2011). doi:10.1175/2011JCLI4137.1
2. IPCC, 2013: Annex I: Atlas of Global and Regional Climate Projections [van Oldenborgh, G. J., M. Collins, J. Arblaster, J. H. Christensen, J. Marotzke, S. B. Power, M. Rummukainen and T. Zhou (eds.)]. In: Climate Change 2013: The Physical Science Basis. Contribution of Working Group I to the Fifth Assessment Report of the Intergovernmental Panel on Climate Change [Stocker, T. F., D. Qin, G.-K. Plattner, M. Tignor, S. K. Allen, J. Boschung, A.

Nauels, Y. Xia, V. Bex and P. M. Midgley (eds.)]. Cambridge University Press, Cambridge, United Kingdom and New York, NY, USA (2013).

3. A. Weisheimer, T. N. Palmer, On the reliability of seasonal climate forecasts. *J. Royal Soc., Interface* **11**, 20131162 (2014). doi.org/10.1098/rsif.2013.1162
4. S. Totz, E. Tziperman, D. Coumou, K. Pfeiffer, J. Cohen, Winter Precipitation Forecast in the European and Mediterranean Regions Using Cluster Analysis. *Geophys. Res. Lett.* **44**, 12,418–12,426 (2017). doi.org/10.1002/2017GL075674
5. A. M. Milner, R. E. L. Collier, K. H. Roucoux, U. C. Müller, J. Pross, S. Kalaitzidis, K. Christanis, P. C. Tzedakis, Enhanced seasonality of precipitation in the Mediterranean during the early part of the Last Interglacial. *Geology* **40**, 919−922 (2012). doi:10.1130/G33204.1
6. J. E. Kutzbach, G. Chen, H. Cheng, R. Edwards, Z. Liu, Potential role of winter rainfall in explaining increased moisture in the Mediterranean and Middle East during periods of maximum orbitally-forced insolation seasonality. *Clim. Dyn*. **42**, 1079−1095 (2014). doi:10.1007/s00382-013-1692-1
7. S. Toucanne, C. M. A. Minto'o, C. Fontanier, M. A. Bassetti, S. J. Jorry, G. Jouet, Tracking rainfall in the northern Mediterranean borderlands during sapropel deposition. *Quat. Sci. Rev*. **129**, 178−195 (2015). doi:10.1016/j.quascirev.2015.10.016
8. M. Stockhecke, A. Timmermann, R. Kipfer, G. H. Haug, O. Kwiecien, T. Friedrich, L. Menviel, T. Litt, N. Pickarski, F. S. Anselmetti, Millennial to orbital-scale variations of drought intensity in the Eastern Mediterranean. *Quat. Sci. Rev*. **133**, 77−95 (2016). doi: 10.1016/ j.quascirev.2015.12.016
9. N. Roberts, M. D. Jones, A. Benkaddour, W. J. Eastwood, M. L. Filippi, M. R. Frogley, H. F. Lamb, M. J. Leng, J. M. Reed, M. Stein, L. Stevens, B. Valero-Garcés, G. Zanchetta, Stable isotope records of Late Quaternary climate and hydrology from Mediterranean lakes: the ISOMED synthesis. *Quat. Sci. Rev*. **27**, 2426−2441 (2008). doi:10.1016/j.quascirev.2008.09.005
10. M. Magny, N. Combourieu-Nebout, J. L. de Beaulieu, V. Bout-Roumazeilles, D. Colombaroli, S. Desprat, A. Francke, S. Joannin, E. Ortu, O. Peyron, M. Revel, L. Sadori, G. Siani, M. A. Sicre, S. Samartin, A. Simonneau, W. Tinner, B. Vannière, B. Wagner, G. Zanchetta, F. Anselmetti, E. Brugiapaglia, E. Chapron, M. Debret, M. Desmet, J. Didier, L. Essallami, D. Galop, A. Gilli, J. N. Haas, N. Kallel, L. Millet, A. Stock, J. L. Turon, S. Wirth, North–south palaeohydrological contrasts in the central Mediterranean during the Holocene: tentative synthesis and working hypotheses. *Clim. Past* **9**, 2043−2071 (2013). doi:10.5194/cp-9-2043-2013
11. P. C. Tzedakis, H. Hooghiemstra, H. Pälike, The last 1.35 million years at Tenaghi Philippon, revised chronostratigraphy and long-term vegetation trends. *Quat. Sci. Rev*. **25,** 3416−3430 (2006). doi:10.1016/j.quascirev.2006.09.002
12. K.-C. Emeis, A. Camerlenghi, J. A. McKenzie, D. Rio, R. Sprovieri, The occurrence and significance of Pleistocene and Upper Pliocene sapropels in the Tyrrhenian Sea. *Mar. Geol.* **100**, 155−182 (1991). doi:10.1016/0025-3227(91)90231-R
13. D. Kroon, I. Alexander, M. Little, L. J. Lourens, A. Matthewson, A. H. F. Robertson, T. Sakamoto, Oxygen isotope and sapropel stratigraphy in the Eastern Mediterranean during the

last 3.2 million years, in *Proceedings of the Ocean Drilling Program. Scientific results*, A. H. F. Robertson, K.-C. Emeis, C. Richter, A. Camerlenghi. Eds. (College Station, Texas, 1998), vol. 160, pp 181−190 (1998).

14. M. Rossignol-Strick, Mediterranean Quaternary sapropels, an immediate response of the African monsoon to variation of insolation. *Palaeogeogr. Palaeoclimatol. Palaeoecol*. **49**, 237−263 (1985). doi:10.1016/0031-0182(85)90056-2

15. E. J. Rohling, G. Marino, K. M. Grant, Mediterranean climate and oceanography, and the periodic development of anoxic events (sapropels). *Earth Sci. Rev*. **143**, 62−97 (2015). doi:10.1016/j.earscirev.2015.01.008

16. P. C. Tzedakis, Seven ambiguities in the Mediterranean palaeoenvironmental narrative. *Quat. Sci. Rev*. **26**, 2042−2066 (2007). doi:10.1016/j.quascirev.2007.03.014

17. J. H. C. Bosmans, S. S. Drijfhout, E. Tuenter, F. J. Hilgen, L. J. Lourens, E. J. Rohling, Precession and obliquity forcing of the freshwater budget over the Mediterranean. *Quat. Sci. Rev.*, **123**, 16−30 (2015). doi:10.1016/j.quascirev.2015.06.008

18. B. Wagner, T. Wilke, A. Francke, C. Albrecht, H. Baumgarten, A. Bertini, N. Combourieu-Nebout, A. Cvetkoska, M. D´Addabbo, T. H. Donders, K. Föller, B. Giaccio, A. Grazhdani, T. Hauffe, J. Holtvoeth, S. Joannin, E. Jovanovska, J. Just, K. Kouli, A. Koutsodendris, S. Krastel, J. H. Lacey, N. Leicher, M. J. Leng, Z. Levkov, K. Lindhorst, A. Masi, A. M. Mercuri, S. Nomade, N. Nowaczyk, K. Panagiotopoulos, O. Peyron, J. M. Reed, E. Regattieri, L. Sadori, L. Sagnotti, B. Stelbrink, R. Sulpizio, S. Tofilovska, P. Torri, H. Vogel, T. Wagner, F. Wagner-Cremer, G. A. Wolff, T. Wonik, G. Zanchetta, X. S. Zhang, The environmental and evolutionary history of Lake Ohrid (FYROM/Albania): Interim results from the SCOPSCO deep drilling project. *Biogeosciences* **14***,* 2033−2054 (2017). doi:10.5194/bg-14-2033-2017

19. C. Albrecht, T. Wilke, Ancient Lake Ohrid: biodiversity and evolution. *Hydrobiologia* **615**, 103−140 (2008). doi:10.1007/s10750-008-9558-y

20. H. Vogel, B. Wagner, G. Zanchetta, R. Sulpizio, P. Rosén, A paleoclimate record with tephrochronological age control for the last glacial-interglacial cycle from Lake Ohrid, Albania and Macedonia. *J. Paleolimnol.* **44**, 295−310 (2010). doi:10.1007/s10933-009-9404-x

21. B. Wagner, T. Wilke, S. Krastel, G. Zanchetta, R. Sulpizio, K. Reicherter, M. J. Leng, A. Grazhdani, S. Trajanovski, A. Francke, K. Lindhorst, Z. Levkov, A. Cvetkoska, J. M. Reed, X. Zhang, J. H. Lacey, T. Wonik, H. Baumgarten, H. Vogel, The SCOPSCO drilling project recovers more than 1.2 million years of history from Lake Ohrid. *Sci. Drill*. **17**, 19−29 (2014). doi:10.5194/sd-17-19-2014

22. A. Francke, B. Wagner, J. Just, N. Leicher, R. Gromig, H. Baumgarten, H. Vogel, J. H.Lacey, L. Sadori, T. Wonik, M. J. Leng, G. Zanchetta, R. Sulpizio, B. Giaccio, Sedimentological processes and environmental variability at Lake Ohrid (Macedonia, Albania) between 637 ka and the present. *Biogeosciences* **13**, 1179−1196 (2016). doi:10.5194/bg-13-1179-2016.

23. J. H. Lacey, M. J. Leng, A. Francke, H. J. Sloane, A. Milodowski, H. Vogel, H. Baumgarten, G. Zanchetta, B. Wagner, Northern Mediterranean climate since the Middle Pleistocene: a

637 ka stable isotope record from Lake Ohrid (Albania/Macedonia). *Biogeosciences* **13**, 1801−1820 (2016). doi:10.5194/bg-13-1801-2016.

24. T. Friedrich, A. Timmermann, M. Tigchelaar, O. E. Timm, A. Ganopolski, Nonlinear climate sensitivity and its implications for future greenhouse warming. *Sci. Adv*. **2** (2016), p. e1501923. doi:10.1126/sciadv.1501923

25. A. Timmermann, T. Friedrich, Late Pleistocene climate drivers of early human migration. *Nature* **538**, 92−95 (2016). doi:10.1038/nature19365

26. L. E. Lisiecki, M. E. Raymo, A Pliocene-Pleistocene stack of 57 globally distributed benthic ∂18O records. *Paleoceanography* **20**, PA1003 (2005). doi:10.1029/2004PA001071

27. H. Cheng, R. L. Edwards, A. Sinha, C. Spötl, L. Yi, S. T. Chen, M. Kelly, G. Kathayat, X. F. Wang, X. L. Li, X. G. Kong, Y. J. Wang, Y. F. Ning, H. W. Zhang, The Asian monsoon over the past 640,000 years and ice age terminations. *Nature* **534**, 640−646 (2016). doi:10.1038/nature20585

28. T. Y. M. Konijnendijk, M. Ziegler, L. J. Lourens, Chronological constraints on Pleistocene sapropel depositions from high-resolution geochemical records of ODP Sites 967 and 968. *Newslett. Stratigr.* **47**, 263−282 (2014). doi:10.1127/0078-0421/2014/0047

29. F. Colleoni, S. Masina, A. Negri, A. Marzocchi, Plio–Pleistocene high–low latitude climate interplay: a Mediterranean point of view. Earth Planet. Sci. Lett. **319–320,** 35−44 (2012). doi:10.1016/j.epsl.2011.12.020

30. B. Martrat, P. Jimenez-Amat, R. Zahn, J. O. Grimalt, Similarities and dissimilarities between the last two deglaciations and interglaciations in the North Atlantic region. *Quat. Sci. Rev.* **99**, 122−134 (2014). doi:10.1016/j.quascirev.2014.06.016

31. R. M. Trigo, T. J. Osborne, J. M. Corte-Real, The North Atlantic Oscillation influence on Europe: climate impacts and associated physical mechanisms. *Clim. Res*. **20**, 9−17 (2002). doi:10.3354/cr020009

32. J. Laskar, P. Robutel, F. Joutel, M. Gastineau, A. C. M. Correia, B. Levrard, A long-term numerical solution for the insolation quantities of the earth. *Astron. Astrophys*. **428**, 261−285 (2004). doi:10.1051/0004-6361:20041335

33. N. Leicher, G. Zanchetta, R. Sulpizio, B. Giaccio, B. Wagner, S. Nomade, A. Francke, P. Del Carlo, First tephrostratigraphic results of the DEEP site record from Lake Ohrid (Macedonia and Albania). *Biogeosciences* **13**, 2151–2178 (2016). doi:10.5194/bg-13-2151-2016

34. V. C. Farmer, The infrared spectra of minerals, edited by: V. C. Farmer, Mineralogical Society Monograph 4, 227 pp, Adlard & Son, Dorking, Surrey, (1974).

35. N. V. Chukanov, Infrared spectra of mineral species. Springer, Dordrecht, Heidelberg, New York, London (2014). doi:10.1007/978-94-007-7128-4

36. S. J. Blott, K. Pye, GRADISTAT: A grain size distribution and statistics package for the analysis of unconsolidated sediments, *Earth Surf. Proc. Land*. **26**, 1237–1248 (2001). doi:10.1002/esp.261.

37. L. Sadori, A. Koutsodendris, K. Panagiotopoulos, A. Masi, A. Bertini, N. Combourieu-Nebout, A. Francke, K. Kouli, S. Joannin, A. M. Mercuri, O. Peyron, P. Torri, B. Wagner, G.

Zanchetta, G. Sinopoli, T. H. Donders, Pollen-based paleoenvironmental and paleoclimatic change at Lake Ohrid (south-eastern Europe) during the past 500 ka. *Biogeosciences* **13**, 1423–1437 (2016). doi:10.5194/bg-13-1423-2016

38. H.-J. Beug, Leitfaden der Pollenbestimmung für Mitteleuropa und angrenzende Gebiete. Verlag Dr. Friedrich Pfeil, München, Germany (2004).

39. R. Cheddadi, G. G. Vendramin, T. Litt, L. François, M. Kageyama, S. Lorentz, J. M. Laurent, J. L. de Beaulieu, L. Sadori, A. Jost, D. Lunt, Imprints of glacial refugia in the modern genetic diversity of Pinus sylvestris. *Global Ecol. Biogeogr*., **15**, 271–282 (2006). doi:10.1111/j.1466-8238.2006.00226.x

40. M. Rossignol-Strick, The Holocene climatic optimum and pollen records of sapropel 1 in the Eastern Mediterranean, 9000–6000 BP. *Quat. Sci Rev*. **18**, 515–530 (1999). doi:10.1016/S0277-3791(98)00093-6

41. D. Langgut, A. Almogi-Labin, M. Bar-Matthews, M. Weinstein-Evron, Vegetation and climate changes in the South Eastern Mediterranean during the Last Glacial–Interglacial cycle (86 ka): new marine pollen record. *Quat. Sci Rev*. **30**, 3960–3972 (2011). doi:10.1016/j.quascirev.2011.10.016

42. N. Combourieu-Nebout, A. Bertini, E. Russo-Ermolli, O. Peyron, S. Klotz, V. Montade, S. Fauquette, J. Allen, F. Fusco, S. Goring, B. Huntley, S. Joannin, V. Lebreton, D. Magri, E. Martinetto, R. Orain, L. Sadori, Climate changes in the central Mediterranean and Italian vegetation dynamics since the Pliocene. *Rev. Palaeobot. Palynol*. **218**, 127–147 (2015). doi:10.1016/j.revpalbo.2015.03.001

43. M. J. Le Bas, R. W. Le Maitre, A. Streckeisen, B. Zanettin, A Chemical Classification of Volcanic Rocks Based on the Total Alkali-Silica Diagram. *J. Petrol*. **27**, 745–750, (1986). doi:10.1093/petrology/27.3.745

44. J. Just, N. R. Nowaczyk, L. Sagnotti, A. Francke, H. Vogel, J. H. Lacey, B. Wagner, Environmental control on the occurrence of high-coercivity magnetic minerals and formation of iron sulfides in a 640 ka sediment sequence from Lake Ohrid (Balkans). *Biogeosciences* **13**, 2093–2109 (2016). doi:10.5194/bg-13-2093-2016.

45. H. Goosse, V. Brovkin, T. Fichefet, R. Haarsma, P. Huybrechts, J. Jongma, A. Mouchet, F. Selten, P.-Y. Barriat, J.-M. Campin, E. Deleersnijder, E. Driesschaert, H. Goelzer, I. Janssens, M.-F. Loutre, M. A. Maqueda, T. Opsteegh, P.-P. Mathieu, G. Munhoven, E. J. Pettersson, H. Renssen, D. M. Roche, M. Schaeffer, B. Tartinville, A. Timmermann, S. L. Weber, Description of the Earth system model of intermediate complexity LOVECLIM version 1.2. *Geosci. Model Dev*. **3**, 603–633 (2010). doi:10.5194/gmd-3-603-2010.

46. J. D. Opsteegh, R. J. Haarsma, F. M. Selten, A. Kattenberg, ECBILT: a dynamic alternative to mixed boundary conditions in ocean models. *Tellus, Ser. A, Dyn. Meterol. Oceanogr*. **50,** 348–367 (1998). doi:10.3402/tellusa.v50i3.14524

47. H. Goosse, T. Fichefet, Importance of ice-ocean interactions for the global ocean circulation: A model study. *J. Geophys. Res*. **104**, 23337–23355 (1999). doi:10.1029/1999JC900215

48. V. Brovkin, A. Ganopolski, Y. Svirezhev, A continuous climate-vegetation classification for use in climate-biosphere studies. *Ecol. Modell.* **101,** 251–261 (1997). doi:10.1016/S0304-3800(97)00049-5

49. A. Timmermann, T. Friedrich, O. E. Timm, M. O. Chikamoto, A. Abe-Ouchi, A. Ganopolski, Modeling obliquity and CO_2 effects on Southern Hemisphere climate during the past 408 ka. *J. Clim*. **27**, 1863–1875 (2014). doi:10.1175/JCLI-D-13-00311.1

50. A. Berger, Long-term variations of daily insolation and quaternary climate change. *J. Atmos. Sci*. **35**, 2362–2367 (1978). doi:10.1175/1520-0469(1978)035<2362:LTVODI>2.0.CO;2

51. D. Lüthi, M. L. Floch, B. Bereiter, T. Blunier, J.-M. Barnola, U. Siegenthaler, D. Raynaud, J. Jouzel, H. Fischer, K. Kawamura, T. F. Stocker. High-resolution carbon dioxide concentration record 650,000-800,000 years before present. *Nature* **453**, 379–382 (2008). doi:10.1038/nature06949

52. EPICA community members, Eight glacial cycles from an Antarctic ice core. *Nature* **429**, 623–628 (2004). doi:10.1038/nature02599

53. A. Ganopolski, R. Calov, The role of orbital forcing, carbon dioxide and regolith in 100 kyr glacial cycles. *Clim. Past*, **7**, 1415–1425 (2011). doi: 10.5194/cp-7-1415-2011

54. A. Matzinger, Z. Spirkovski, S. Patceva, A. Wüest Sensitivity of ancient Lake Ohrid to local anthropogenic impacts and global warming, *J. Great Lakes Res*. **32**, 158–179 (2006). doi:10.3394/0380-1330(2006)32[158:SOALOT]2.0.CO;2

55. N. Hoffmann, K. Reicherter, T. Fernández-Steeger, C. Grützner, Evolution of ancient Lake Ohrid: a tectonic perspective, Biogeosciences **7**, 3377–3386 (2010). doi:10.5194/bg-7-3377-2010

56. C. Popovska, O. Bonacci, Basic data on the hydrology of Lakes Ohrid and Prespa. *Hydrol. Process*. **21**, 658–664 (2007). doi:10.1002/hyp.6252

57. I. Kousis, A. Koutsodendris, O. Peyron, N. Leicher, A. Francke, B. Wagner, B. Giaccio, M. Knipping, J. Pross, Centennial-scale vegetation dynamics and climate variability in SE Europe during Marine Isotope Stage 11 based on a pollen record from Lake Ohrid. *Quat. Sci. Rev*. **190**, 20−38 (2018). doi:10.1016/j.quascirev.2018.04.014

58. B. Giaccio, P. Messina, A. Sposato, M. Voltaggio, G. Zanchetta, F.,Galadini, S. Gori, R. Santacroce, Tephra layers from Holocene lake sediments of the Sulmona Basin, Central Italy: implications for volcanic activity in Peninsular Italy and tephrostratigraphy in the Central Mediterranean area. *Quat. Sci. Rev*. **28**, 2710−2733 (2009). doi:10.1016/j.quascirev.2009.06.009

59. B. Giaccio, F. Castorina, S. Nomade, G. Scardia, M. Voltaggio, L. Sagnotti, Revised Chronology of the Sulmona Lacustrine Succession, Central Italy. *J. Quat. Sci.* **28**, 545−551 (2013b). doi:10.1002/jqs.2647

60. N. Ciaranfi, F. Lirer, L. Lirer, L. J. Lourens, P. Maiorano, M. Marino, P. Petrosino, M. Sprovieri, S. Stefanelli, M. Brilli, A. Girone, S. Joannin, N. Pelosi, M. Vallefuoco, Integrated stratigraphy and astronomical tuning of Lower–Middle Pleistocene Montalbano Jonico section (Southern Italy). *Quat. Internat.* **219**, 109−120 (2010). doi:10.1016/j.quaint.2009.10.027

61. P. Petrosino, B. R. Jicha, F. C. Mazzeo, N. Ciaranfi, A. Girone, P. Maiorano, M. Marino, The Montalbano Jonico marine succession: An archive for distal tephra layers at the Early–

Middle Pleistocene boundary in southern Italy. *Quat. Internat*. **383**, 89−103 (2015). doi:10.1016/j.quaint.2014.10.049

62. F. Massari, D. Rio, M. Sgavetti, G. Prosser, A. D'Alessandro, A. Asioli, L. Capraro, E. Fornaciari F. Tateo, Interplay between tectonics and glacio-eustasy: Pleistocene succession of the Crotone basin, Calabria (southern Italy). *Geol. Soc. Am. Bull*. **114**, 1183−1209 (2002). doi:10.1130/0016-7606(2002)114<1183:IBTAGE>2.0.CO;2

63. L. Capraro, A. Asioli, J. Backman, R. Bertoldi, J. E. T. Channell, F. Massari, D. Rio, Climatic patterns revealed by pollen and oxygen isotope records across the Matuyama-Brunhes Boundary in the central Mediterranean (southern Italy). *Geol. Soc., London, Spec. Publ*. **247**, 159−182 (2005). doi:10.1144/GSL.SP.2005.247.01.09

64. L. Capraro, F. Massari, D. Rio, E. Fornaciari, J. Backman, J. E. T. Channell, P. Macrì, G. Prosser, F. Speranza, Chronology of the Lower–Middle Pleistocene succession of the south-western part of the Crotone Basin (Calabria, Southern Italy). *Quat. Sci. Rev*. **30**, 1185−1200 (2011). doi:10.1016/j.quascirev.2011.02.008

65. B. Giaccio, P. Galli, E. Peronace, I. Arienzo, S. Nomade, G. P. Cavinato, M. Mancini, P. Messina, Sottili, G., A 560-440 ka tephra record from the Mercure Basin, Southern Italy: volcanological and tephrostratigraphic implications. *J. Quat. Sci.* **29**, 232−248 (2014). doi:10.1002/jqs.2696

66. B. Giaccio, E. Regattieri, G. Zanchetta, S. Nomade, P.R. Renne, C. J. Sprain, R. N. Drysdale, P. C. Tzedakis, P. Messina, G. Scardia, A. Sposato, F. Bassinot, Duration and dynamics of the best orbital analogue to the present interglacial. *Geology* **43**, 603−606 (2015). doi:10.1130/G36677.1

67. L. Sagnotti, G. Scardia, B. Giaccio, J. C. Liddicoat, S. Nomade, P. R. Renne, C. J. Sprain, Extremely rapid directional change during Matuyama-Brunhes geomagnetic polarity reversal. *Geophys. J. Internat*. **199**, 1110−1124 (2014). doi:10.1093/gji/ggu287

68. L. Sagnotti, B. Giaccio, J. C. Liddicoat, S. Nomade, P. R. Renne, G. Scardia, C. J. Sprain, How fast was the Matuyama–Brunhes geomagnetic reversal? A new subcentennial record from the Sulmona Basin, central Italy. *Geophys. J. Internat*. **204**, 798−812 (2016). doi:10.1093/gji/ggv486

69. Q. Simon, D. L. Bourlès, F. Bassinot, S. Nomade, M. Marino, N. Ciaranfi, A. Girone, P. Maiorano, N. Thouveny, S. Choy, F. Dewilde, V. Scao, G. Isguder, D. Blamart, Authigenic 10Be/9Be ratio signature of the Matuyama–Brunhes boundary in the Montalbano Jonico marine succession. *Earth Planet. Sci. Lett.* **460**, 255−267 (2017). doi:10.1016/j.epsl.2016.11.052

70. D. Rio, J. E. T. Channell, F. Massari, M. S. Poli, M. Sgavetti, A. D'Alessandro, G. Prosser, Reading Pleistocene eustasy in a tectonically active siliciclastic shelf setting (Crotone peninsula, southern Italy). *Geology* **24**, 743−746 (1996). doi:10.1130/0091-7613(1996)024<0743:RPEIAT>2.3.CO;2

71. P. Macrì, L. Capraro, P. Ferretti, D. Scarponi, A high-resolution record of the Matuyama-Brunhes transition from the Mediterranean region: The Valle di Manche section (Calabria, Southern Italy). *Phys. Earth Planet Inter.* **278**, 1−15 (2018). doi:10.1016/j.pepi.2018.02.005

72. B. Giaccio, I. Hajdas, R. Isaia, A. Deino, S. Nomade, High-precision 14C and 40Ar/39Ar dating of the Campanian Ignimbrite (Y-5) reconciles the time-scales of climatic-cultural processes at 40 ka. *Sci. Rep.* **7**, 45940 (2017a). doi:10.1038/srep45940

73. E. Regattieri, B. Giaccio, S. Nomade, A. Francke, H. Vogel, R. N. Drysdale, N. Perchiazzi, B. Wagner, M. Gemelli, I. Mazzini, C. Boschi, P. Galli, E. Peronace, A Last Interglacial record of environmental changes from the Sulmona Basin (central Italy). *Palaeogeogr. Palaeoclimatol. Palaeoecol*. **472**, 51−66 (2017). doi:10.1016/j.palaeo.2017.02.013

74. B. Giaccio, E. M. Niespolo, A. Pereira, S. Nomade, P. R. Renne, P. G. Albert, I. Arienzo, E. Regattieri, B. Wagner, G. Zanchetta, M. Gaeta, P. Galli, G. Mannella, E. Peronace, G. Sottili, F. Florindo, N. Leicher, F. Marra, E. L. Tomlinson, First integrated tephrochronological record for the last ~190 kyr from the Fucino Quaternary lacustrine succession, central Italy. *Quat. Sci. Rev*. **158**, 211−234 (2017b). doi:10.1016/j.quascirev.2017.01.004

75. M. A. Laurenzi, I. Villa, $^{40}Ar/^{39}Ar$ chronostratigraphy of Vico ignimbrites. *Period. Mineral.* **56**, 285−293 (1987).

76. D. B. Karner, F. Marra, P. R. Renne, The history of the Monti Sabatini and Alban Hills volcanoes: groundwork for assessing volcanic-tectonic hazards for Rome. *J. Volcanol. Geotherm. Res.* **107**, 185−219 (2001). doi: 10.1016/S0377-0273(00)00258-4

77. P. R. Renne, G. Balco, K. R. Ludwig, R. Mundil and K. Min, Response to the comment by W. H. Schwarz et al. on "Joint determination of 40 K decay constants and 40 Ar∗/40 K for the Fish Canyon sanidine standard, and improved accuracy for 40 Ar/39 Ar geochronology" by P. R. Renne et al. (2010). *Geochim. Cosmochim. Acta* **75**, 5097−5100 (2011). doi:10.1016/j.gca.2010.06.017

78. E. M. Niespolo, D. Rutte, A. L. Deino, P. R. Renne, Intercalibration and age of the Alder Creek sanidine 40 Ar/ 39 Ar standard. *Quat. Geochronol*. **39**, 205−213 (2017). doi:10.1016/j.quageo.2016.09.004

79. C. M. Mercer, K.V. Hodges, ArAR — A software tool to promote the robust comparison of K–Ar and 40Ar/39Ar dates published using different decay, isotopic, and monitor-age parameters. *Chem. Geol*. **440**, 148−163 (2016). doi:10.1016/j.chemgeo.2016.06.020

80. M. Blaauw, J. A. Christen, Flexible paleoclimate age-depth models using an autoregressive gamma process. *Bayes. Analys*. **6**, 457−474 (2011). doi:10.1214/ba/1339616472

81. O. Hammer, PAleontological Statistics (PAST) Version 3.21 reference manual, Natural History Museum, University of Oslo (2018). https://folk.uio.no/ohammer/past/

82. C. Torrence, G. P. Compo. A practical guide to wavelet analysis. *Bull. Am. Meteorol. Soc.* **79**, 61−78. (1998). doi:10.1175/1520-0477(1998)079<0061:APGTWA>2.0.CO;2

83. K. Lindhorst, S. Krastel, K. Reicherter, M. Stipp, B. Wagner, T. Schwenk, Sedimentary and tectonic evolution of Lake Ohrid (Macedonia/Albania). *Basin Res*. **27**, 84−101 (2015). doi:10.1111/bre.12063

84. G. Zanchetta, E. Regattieri, B. Giaccio, B. Wagner, R. Sulpizio, A. Francke, H. Vogel, L. Sadori, A. Masi, G. Sinopoli, J. H. Lacey, M. J. Leng, N. Leicher, Aligning and synchronization of MIS5 proxy records from Lake Ohrid (FYROM) with independently

dated Mediterranean archives: implications for DEEP core chronology. *Biogeosciences*, **13**, 2757–2768 (2016). doi:10.5194/bg-13-2757-2016

85. G. Melard, Algorithm AS 197: A fast algorithm for the exact likelihood of autoregressive-moving average models. *Appl. Stat.* **33**,104–114 (1984). doi:10.2307/2347672

86. B. Giaccio, I. Arienzo, G. Sottili, F. Castorina, M. Gaeta, S. Nomade, P. Galli, P. Messina, Isotopic (Sr-Nd) and major element fingerprinting of distal tephras: an application to the Middle-Late Pleistocene markers from the Colli Albani volcano, central Italy. *Quat. Sci. Rev*. 67, 190–206 (2013a).doi: 10.1016/j.quascirev.2013.01.028

87. G. Zanchetta, R. Sulpizio, N. Roberts, R. Cioni, W. J. Eastwood, G. Siani, B. Caron, M. Paterne, R. Santacroce, Tephrostratigraphy, chronology and climatic events of the Mediterranean basin during the Holocene: An overview. *Holocene* **21**, 33–52 (2011). doi:10.1177/0959683610377531

88. P. G. Albert, M. Hardiman, J. Keller, E. L. Tomlinson, V. C. Smith, A. J. Bourne, S. Wulf, G. Zanchetta, R. Sulpizio, U. C. Müller, J. Pross, L. Ottolini, I. P. Matthews, S. P. E. Blockley, M. A. Menzies, Revisiting the Y-3 tephrostratigraphic marker: a new diagnostic glass geochemistry, age estimate, and details on its climatostratigraphical context, *Quat. Sci. Rev*. **118**, 105–121 (2015). doi:10.1016/j.quascirev.2014.04.002

89. C. Satow, E. L. Tomlinson, K. M. Grant, P. G. Albert, V. C. Smith, C. J. Manning, L. Ottolini, S. Wulf, E. J. Rohling, J. J. Lowe, S. P. E. Blockley, M. A. Menzies, A new contribution to the Late Quaternary tephrostratigraphy of the Mediterranean: Aegean Sea core LC21, *Quat. Sci. Rev*. **117**, 96–112 (2015). doi:10.1016/j.quascirev.2015.04.005

90. P. Petrosino, B. R. Jicha, F. C. Mazzeo, E. Russo Ermolli, A high resolution tephrochronological record of MIS 14–12 in the Southern Apennines (Acerno Basin, Italy). *J. Volcanol. Geotherm. Res*. **274**, 34–50 (2014). doi:10.1016/j.jvolgeores.2014.01.014

91. F. Marra, D. B. Karner, C. Freda, M. Gaeta, P. Renne, Large mafic eruptions at Alban Hills Volcanic District (Central Italy): Chronostratigraphy, petrography and eruptive behavior. *J. Volcanol. Geotherm. Res*. **179**, 217–232 (2009). doi:10.1016/j.jvolgeores.2008.11.009

Acknowledgments: The Hydrobiological Institute in Ohrid (S. Trajanovski and G. Kostoski) and the Hydrometeorological Institute in Tirana (M. Sanxhaku and B. Lushaj) provided logistic support for pre-site surveys and the deep drilling campaign. Drilling was carried out by Drilling, Observation and Sampling of the Earth's Continental Crust (DOSECC) and using the Deep Lake Drilling System (DLDS). **Funding:** The SCOPSCO Lake Ohrid drilling project was funded by the International Continental Scientific Drilling Program (ICDP), the German Ministry of Higher Education and Research, the German Research Foundation, the University of Cologne, the British Geological Survey, the INGV and CNR (both Italy), and the governments of the republics of Macedonia. (FYROM) and Albania. **Author contributions:** B Wagner and H Vogel designed the study and contributed equally. BW initiated and coordinated the SCOPSCO drilling project and drilling campaign. HV conceived major scientific ideas of the study. A Francke, T Friedrich, T Donders, J Lacey, M Leng, E Regattieri, L Sadori, T Wilke and G Zanchetta contributed key datasets, interpretations, and oversaw the generation of data used in the study.

Data, discussion and interpretation were provided by A Bertini (pollen, MIS 19-21, MIS 25-28), N Combourieu-Nebout (pollen, MIS 1-4, MIS 8, MIS 14-15), B Giaccio (tephrostratigraphy), S Joannin (pollen, MIS 1-4, MIS 13-16, MIS 30), J Just (paleomagnetic data), K Kouli (pollen, MIS 6-8, MIS 10, MIS 16-19, MIS 28-30, MIS 33), I Kousis (pollen, MIS 11-12, MIS 15), A Koutsodendris (pollen, MIS 11-12, MIS 15), N Leicher (tephrostratigraphy), A Masi (pollen, MIS 5-6, MIS 20-25, MIS 31-32), A M Mercuri (pollen, MIS 6, MIS 34), S Nomade (tephrochronology), N Nowaczyk (paleomagnetic data), K Panagiotopoulos (pollen, MIS 7-8, MIS 35-43), O. Peyron (pollen, MIS 1-4, MIS 13-16, MIS 30), L Sagnotti (paleomagnetic data), G Sinopoli (pollen, MIS 5-6) and P Torri (pollen MIS 6, MIS 34). All other authors contributed to the discussion and interpretation of the data and provided comments and suggestions to the manuscript. **Competing interests:** Authors declare no competing interests. **Data and materials availability:** Data is available in the main text, in the supplementary materials and in the pangaea database. Data used g´for LOVECLIM are available at https://climatedata.ibs.re.kr/grav/data/loveclim-784k.

Fig. 1.

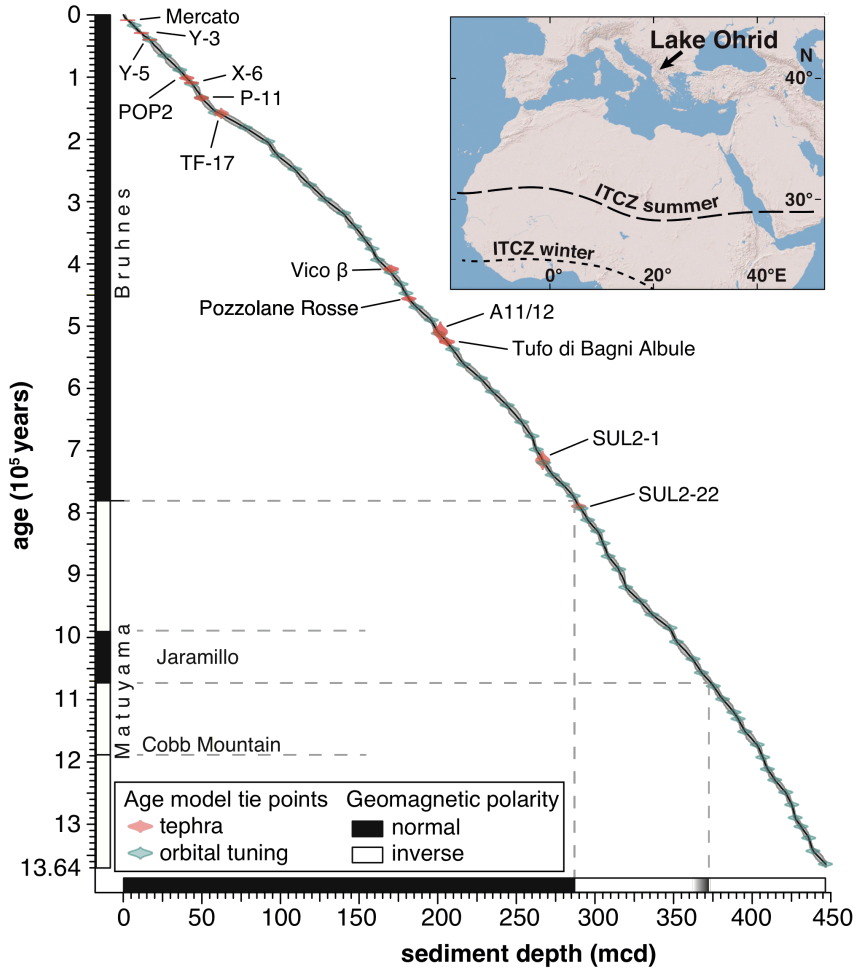

Fig. 1. Age model of the DEEP site record. The age model is based on tephrochronological correlation of 13 tephra layers (red, first-order tie points), two paleomagnetic age reversals (dashed lines, first-order tie points) and tuning of total organic carbon (TOC) minima in the DEEP site record vs. inflection points in insolation and winter season length (blue, second-order tie points). Ages and errors of the tephra layers and the age model are discussed in detail in the Supplementary information. The insert shows the location of Lake Ohrid in the Balkans and the approximate position of the intertropical convergence zone (ITCZ) in summer and winter.

Fig. 2.

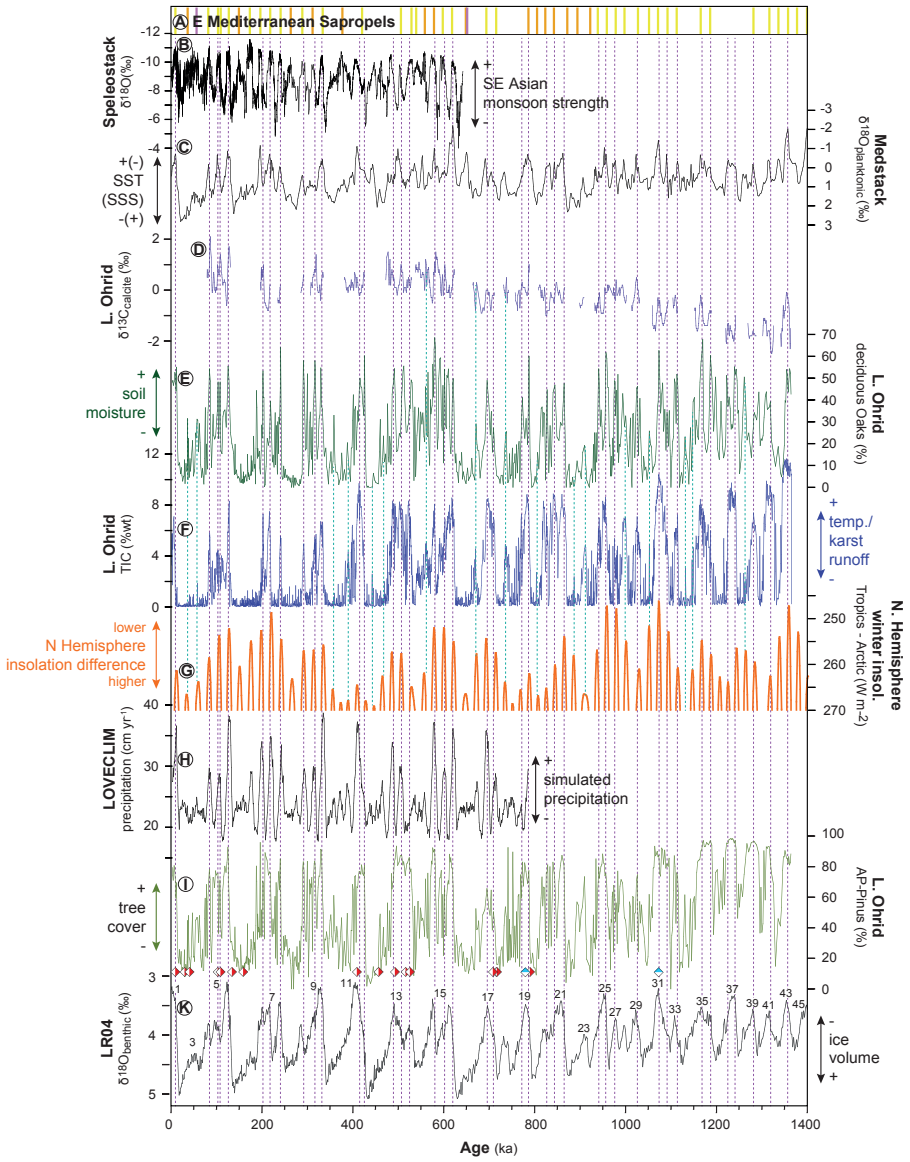

Fig. 2. Lake Ohrid rainfall indicators and global monsoon records for the last 1.4 million years. **(A)** Eastern Mediterranean Sapropel ages (green = sapropel, red = red interval/oxidized sapropel, violet = ghost sapropel; *12*, *13*, *28*); **(B)** Chinese Speleostack $\delta^{18}O$ (*27*); **(C)** Medstack $\delta^{18}O$ planktonic (*29*); SST = sea surface temperature, SSS = sea surface salinity; **(D)** Lake Ohrid $\delta^{13}C$ endogenic calcite; **(E)** Lake Ohrid deciduous oaks pollen percentage; **(F)** Lake Ohrid total inorganic carbon (TIC) concentrations; **(G)** Northern Hemisphere winter insolation difference between the tropic of cancer and the arctic circle (*32*); **(H)** annual mean precipitation amount for the Lake Ohrid grid cell from the LOVECLIM simulation; **(I)** Lake Ohrid arboreal pollen excluding pinus pollen (AP-P) percentages; **(K)** LR04 benthic $\delta^{18}O$ stack (*26*) odd numbers indicate interglacials; red and white diamonds indicate the position of radiometrically dated tephra layers, blue and white diamonds the position of reversals of Earth's magnetic field in the Lake Ohrid sediment record.

Fig. 3.

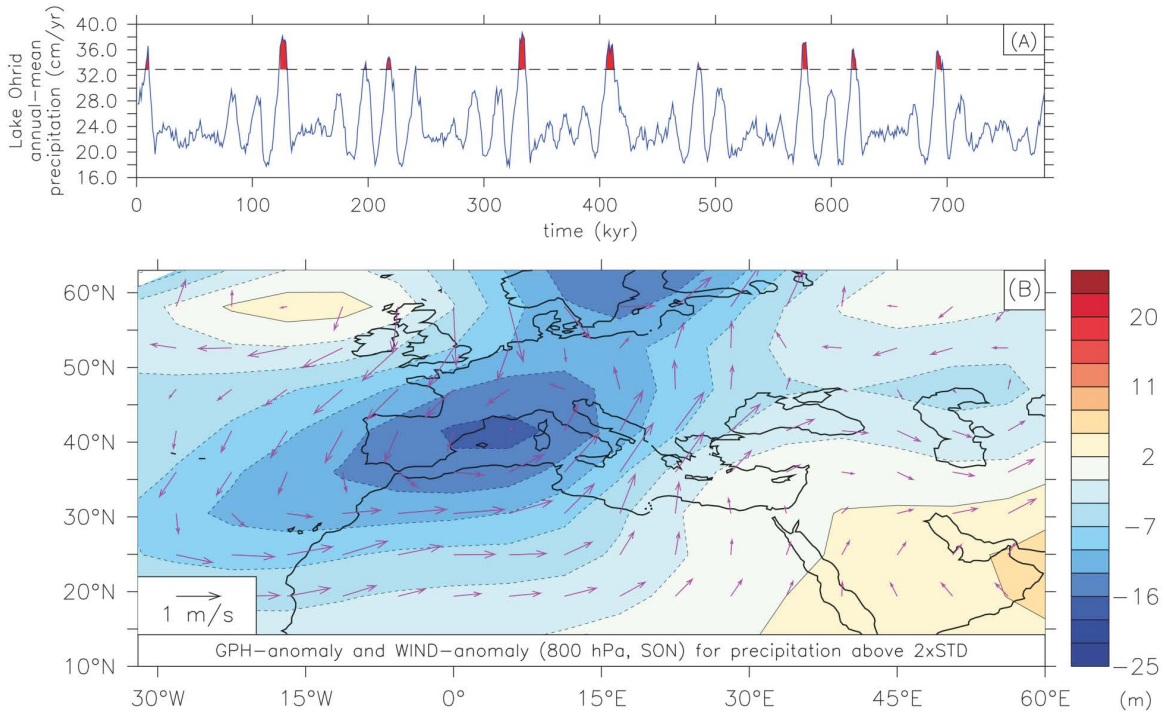

Fig. 3. Simulated Lake Ohrid precipitation and atmospheric anomaly pattern associated with precipitation maxima. (A) Simulated precipitation (cm yr^{-1}) for the Lake Ohrid grid cell. Data based on 1000-year averages. Dashed line indicates two standard deviations above the mean. Red shading highlights precipitation values exceeding two standard deviations. See Methods for details on the model simulations. **(B)** Composite anomalies of September-November (SON), 800 hPa geopotential height (m, shading) and wind (m s^{-1}, vectors) associated with precipitation maxima shown in (A).